Supplementary Information

Loss of adipose ATF3 promotes adipose tissue lipolysis and the development of MASH

Shuwei Hu, Fathima N. Cassim Bawa, Yingdong Zhu, Xiaoli Pan, Hui Wang, Raja Gopoju, Yanyong Xu, Yanqiao Zhang

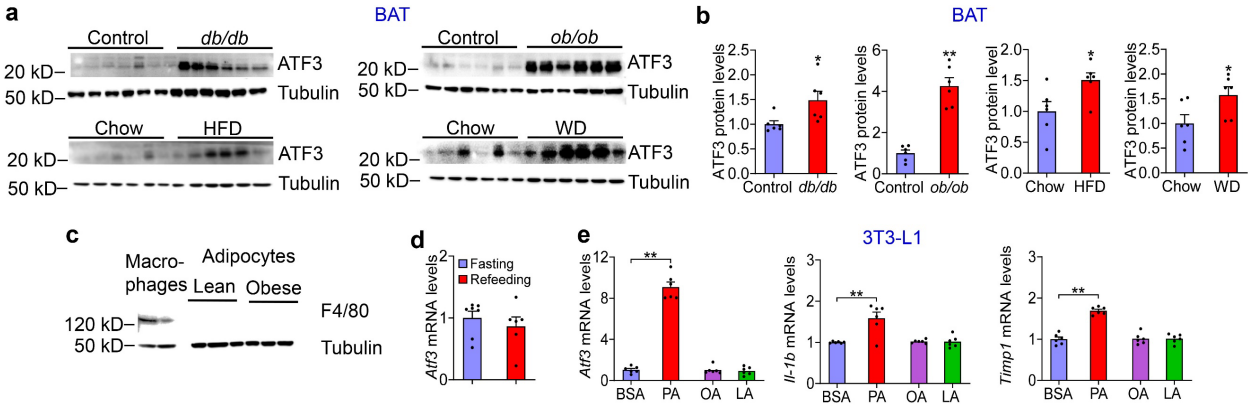

Supplementary Fig. 1. ATF3 tissue distribution and regulation under different nutritional status. a-b ATF3 protein levels in BAT of *db/db*, *ob/ob,* high fat diet (HFD)-fed or Western diet (WD)-fed mice, and their control mice (n=6 per group). **c** Adipocytes were isolated from male C57BL/6 mice that had been fed a chow diet (lean) or Western diet (obese) for 4 months. Western blot assays were performed. Protein lysates from macrophages served as a positive control. **d** Male C57BL/6J mice were randomly split into two groups: fasting (24-h fast) and refeeding (24-h fast followed by a 6-h re-feeding). *Atf3* mRNA levels in the liver were quantified (n=6-7). **e** 3T3-L1 cells were treated with DMEM containing IBMX/Dex/Insulin for 2 days, and the media were then changed to DMEM containing Dex/Insulin every 2 days until fully differentiated. After culture in DMEM without FBS for 3 h, the cells were treated with bovine serum albumin (BSA; control) or 100 μM palmitic acid (PA), oleic acid (OA), or linoleic acid (LA) for 24 h, and related mRNA levels were quantified (n=6 per group). Data are expressed as mean±SEM. Statistical analysis was performed using a 2-tailed, unpaired *t*-test (**b, d**) or one-way ANOVA (**e**). **P*<0.05, ***P*<0.01 versus controls

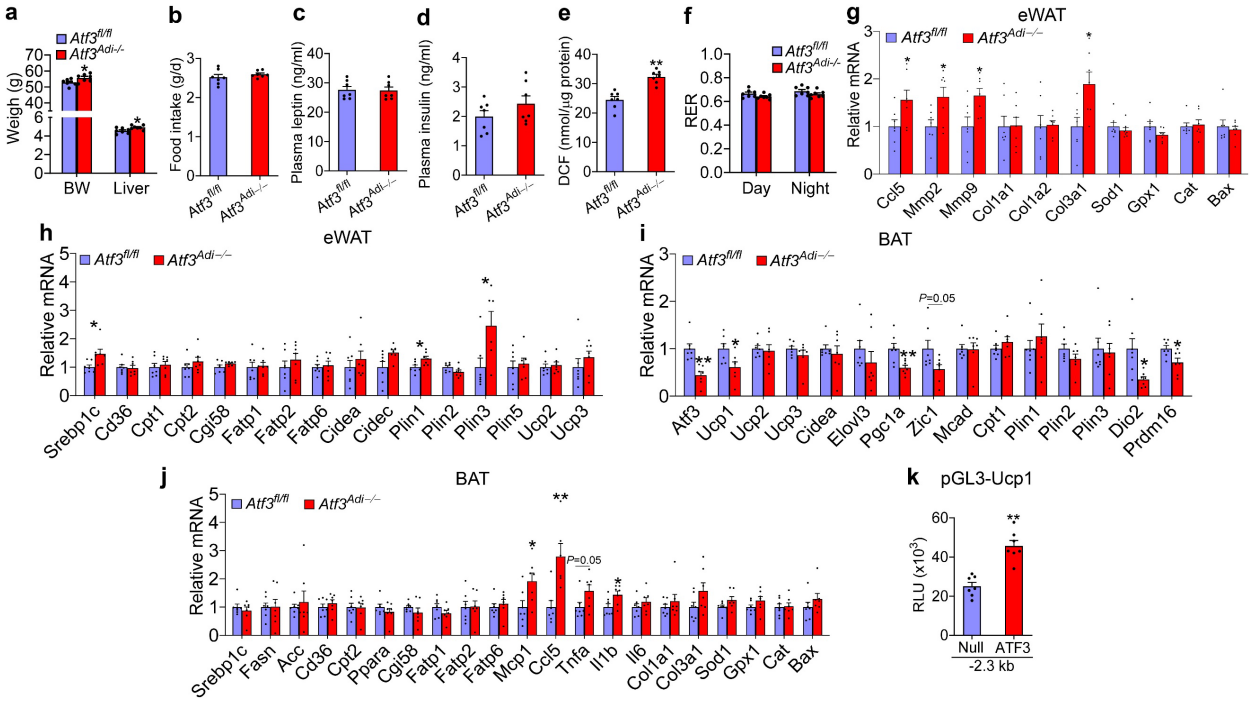

Supplementary Fig. 2. Effect of loss of adipocyte ATF3 on body weight, food intake, liver and plasma biochemistry, and hepatic or adipose gene expression in Western diet-fed mice. *Aft3*$^{fl/fl}$ mice and *Atf3*$^{Adi-/-}$ mice were fed a western diet (WD) for 20 weeks (n=7 per group). **a** Body or liver weight. **b** Food intake. **c** Plasma leptin levels. **d** Plasma insulin levels. **e** Hepatic ROS levels. **f** RER. (**g-j**) mRNA levels in eWAT (**g-h**) or BAT (**i-j**). **k** Transient transfections were performed in 3T3-L1 cells using the *Ucp1* promoter-luciferase construct together with CMV-Null or CMV-ATF3 (n=7). Data are expressed as mean±SEM. Statistical analysis was performed using a 2-tailed, unpaired *t*-test (**a-e, g-k**) or two-way ANOVA (**f**) **P*<0.05, ***P*<0.01 versus controls

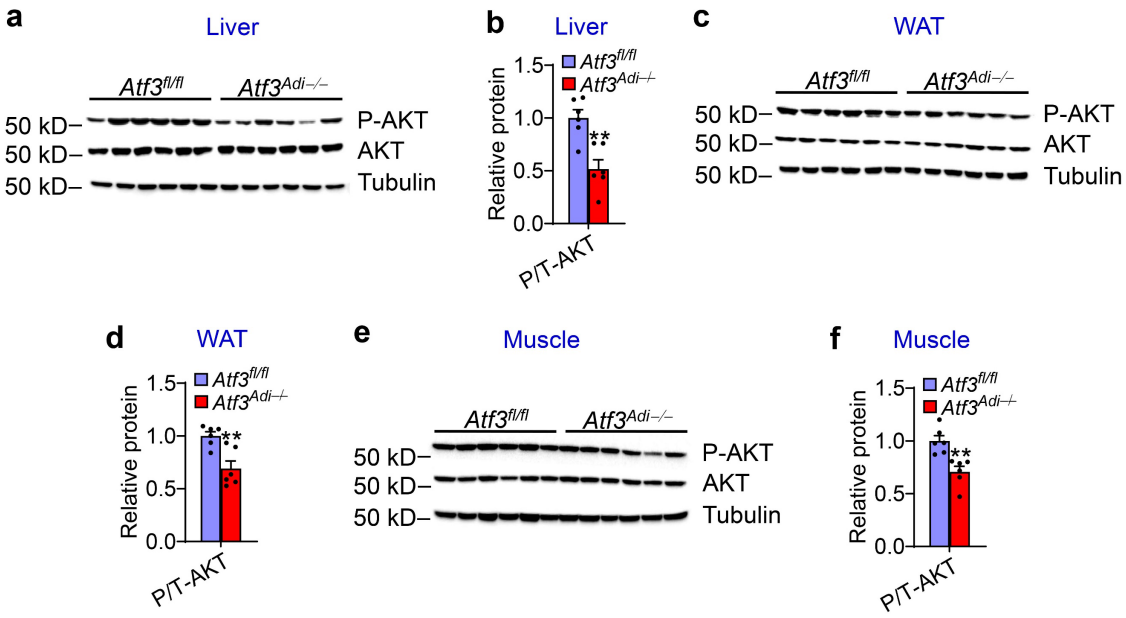

Supplementary Fig. 3. Loss of adipocyte ATF3 inhibits insulin signaling in the liver and adipose tissue. *Aft3*$^{fl/fl}$ mice and *Atf3*$^{Adi-/-}$ mice were fed a western diet (WD) for 12 weeks (n=7 per group). Mice were fasted for 6 h followed by an i.p. injection of 1 U/kg insulin. After 15 min, liver and adipose tissue were collected. **a-b** P-AKT levels in the liver. **c-d** P-AKT levels in WAT. **e-f** P-AKT levels in skeletal muscle. Data are expressed as mean±SEM. Statistical analysis was performed using a 2-tailed, unpaired *t*-test (**b, d, f**). ***P*<0.01 versus controls

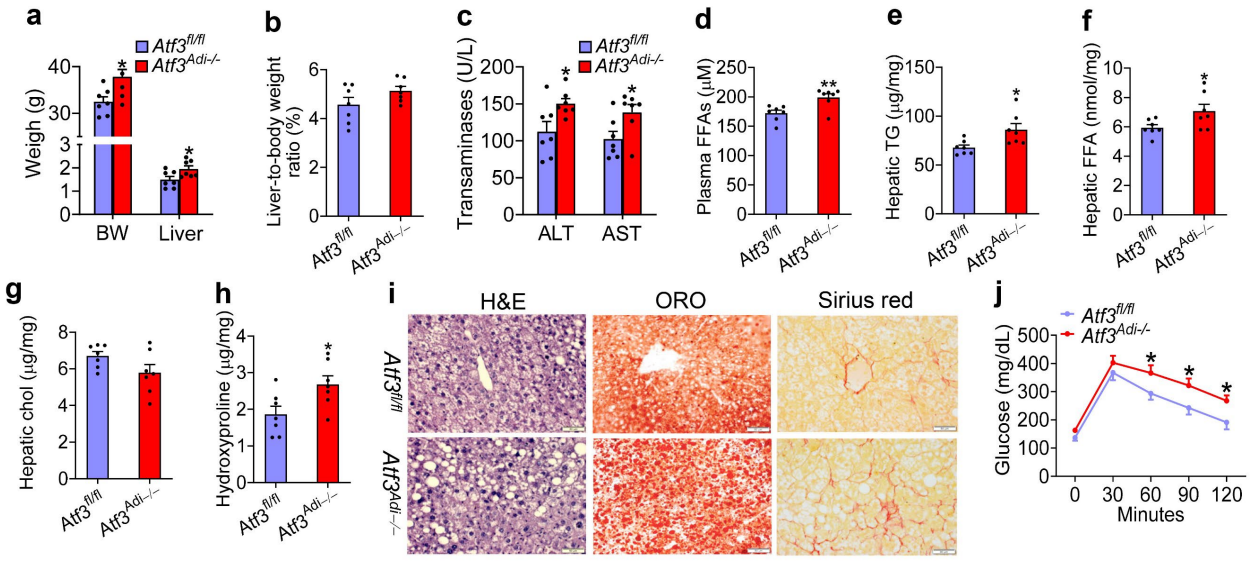

Supplementary Fig. 4. Loss of adipocyte ATF3 aggravates steatohepatitis when fed a Western diet for 10 weeks. *Aft3*$^{fl/fl}$ mice and *Atf3*$^{Adi-/-}$ mice were fed a Western diet for 10 weeks (n=7 per group). **a** Body or liver weight. **b** Liver-to-body weight ratio. **c** Plasma AST or ALT levels. **d** Plasma free fatty acid (FFA) levels. **e** Hepatic triglyceride (TG) levels. **f** Hepatic FFA levels. **g** Hepatic cholesterol levels. **h** Hepatic hydroxyproline levels. **i** Hematoxylin (H&E) staining (left panel), Oil red O (ORO) staining (middle panel), and picrosirius red staining (right panel). **j** Glucose tolerance test (GTT). Scale bar in **i**: 50 μm. Data are expressed as mean±SEM. Statistical analysis was performed using a 2-tailed, unpaired *t*-test (**a**-**h**) or two-way ANOVA (**j**). **P*<0.05, ***P*<0.01 versus controls

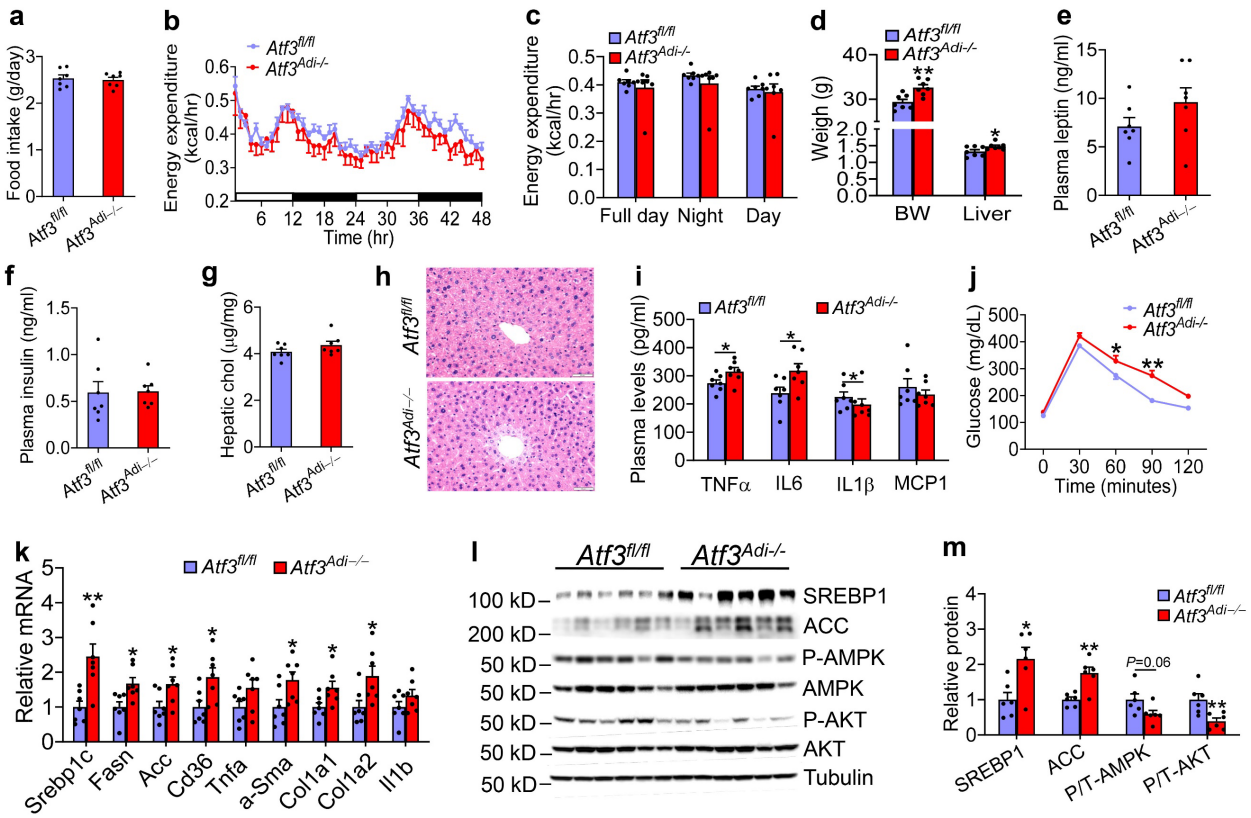

Supplementary Fig. 5. Effect of adipocyte ATF3 ablation on metabolic homeostasis and hepatic gene expression in chow diet-fed mice. *Aft3*$^{fl/fl}$ mice and *Atf3*$^{Adi-/-}$ mice were fed a chow diet (n=7 per group) for 16 weeks. **a** Food intake. (**b-c**) Energy expenditure during the day or night time. **d** liver or body weight. **e** Plasma leptin levels. **f** Plasma insulin levels. **g** Hepatic cholesterol levels. **h** H&E staining of liver sections. **i** Plasma cytokine levels. **j** Glucose tolerance test. (**k-m**) Hepatic mRNA (**k**) or protein (**l-m**) levels. Scar bars in **h**: 50 μm. Data are expressed as mean±SEM. Statistical analysis was performed using a 2-tailed, unpaired t-test (**a, d-g, i, k, m)** or two-way ANOVA (**b-c, j**). **P*<0.05, ***P*<0.01

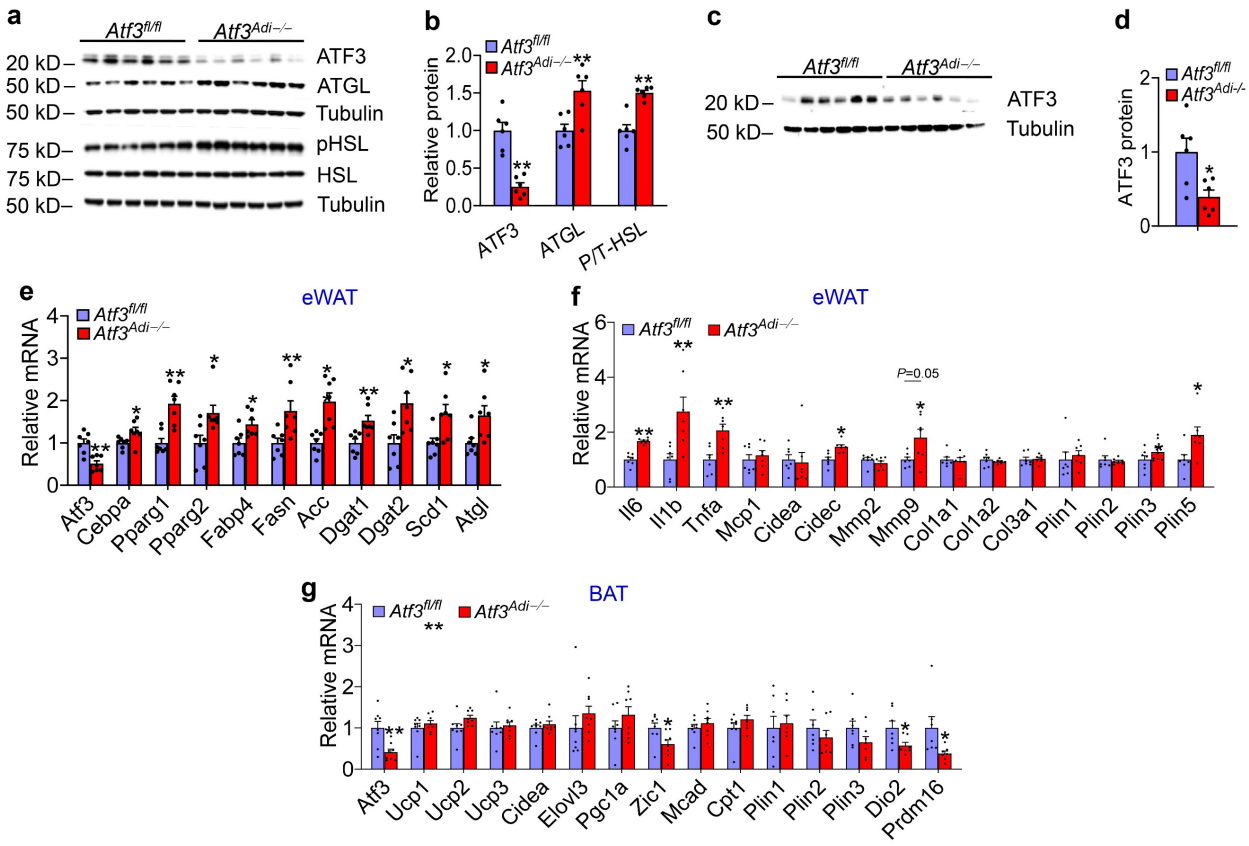

Supplementary Fig. 6. Effect of adipocyte ATF3 ablation on adipose gene expression in chow-fed mice. *Aft3*$^{fl/fl}$ mice and *Atf3*$^{Adi-/-}$ mice were fed a chow diet for 16 weeks (n=7 per group). **a-b** Protein levels in eWAT. **c-d** Protein levels in BAT. **e-f** mRNA levels in eWAT. **g** mRNA levels in BAT. Data are expressed as mean±SEM. Statistical analysis was performed using a 2-tailed, unpaired *t*-test (**b, d, e-g**). **P*<0.05, ***P*<0.01 versus controls

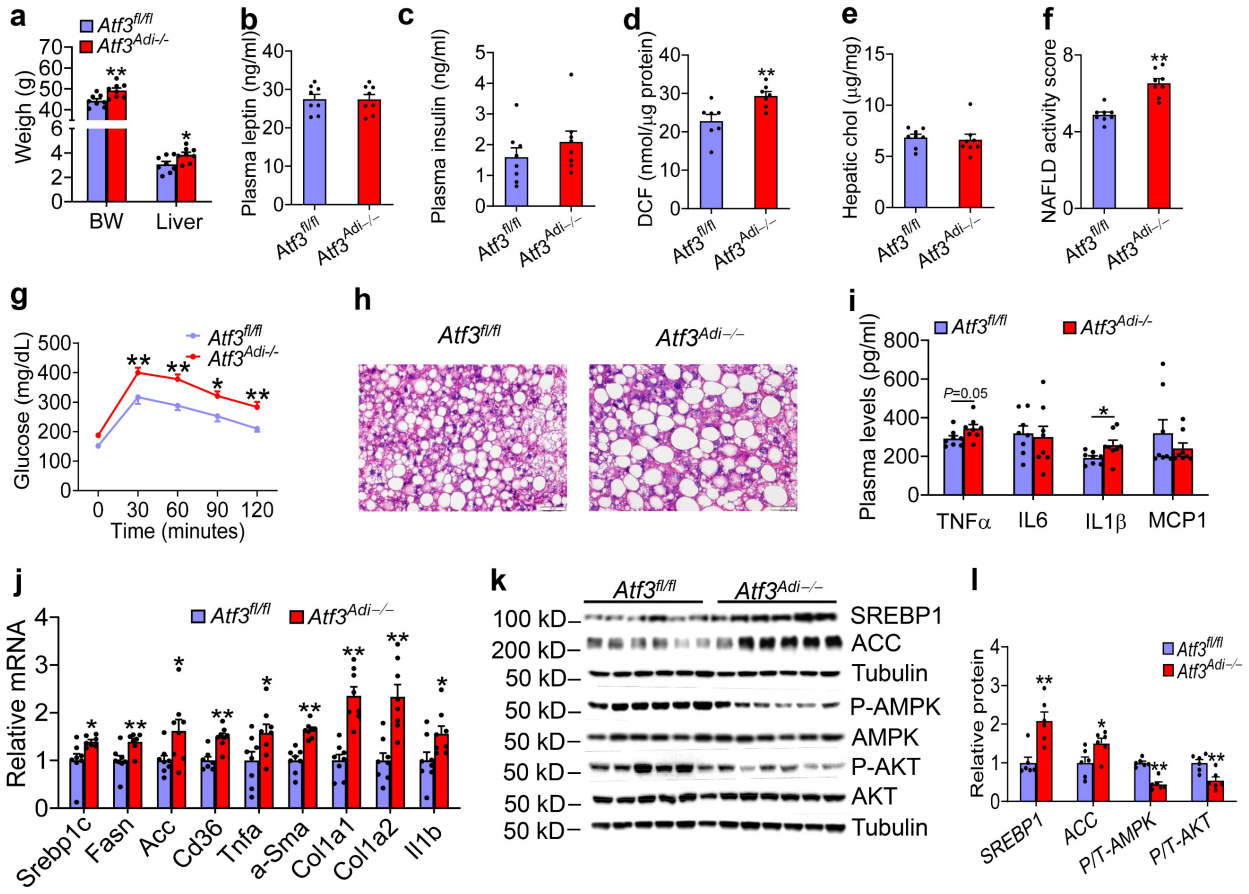

Supplementary Fig. 7. Effect of adipocyte ATF3 ablation on metabolic homeostasis and hepatic gene expression in high fat diet-fed mice. *Aft3*$^{fl/fl}$ mice and *Atf3*$^{Adi-/-}$ mice were fed a high fat diet (HFD) for 16 weeks (n=8 per group). **a** Body or liver weight. **b** Plasma leptin levels. **c** Plasma insulin levels. **d** Hepatic reactive oxygen species (ROS) levels. **e** Hepatic cholesterol levels. **f** NAFLD activity score. **g** Glucose tolerance test. **h** H&E staining of liver sections. **i** Plasma cytokine levels (**j-l**) Hepatic mRNA (**j**) and protein (**k-l**) levels. Data are expressed as mean±SEM. Statistical analysis was performed using a 2-tailed, unpaired t-test (**a-f, i-j, l**) or two-way ANOVA (**g**). **P*<0.05, ***P*<0.01

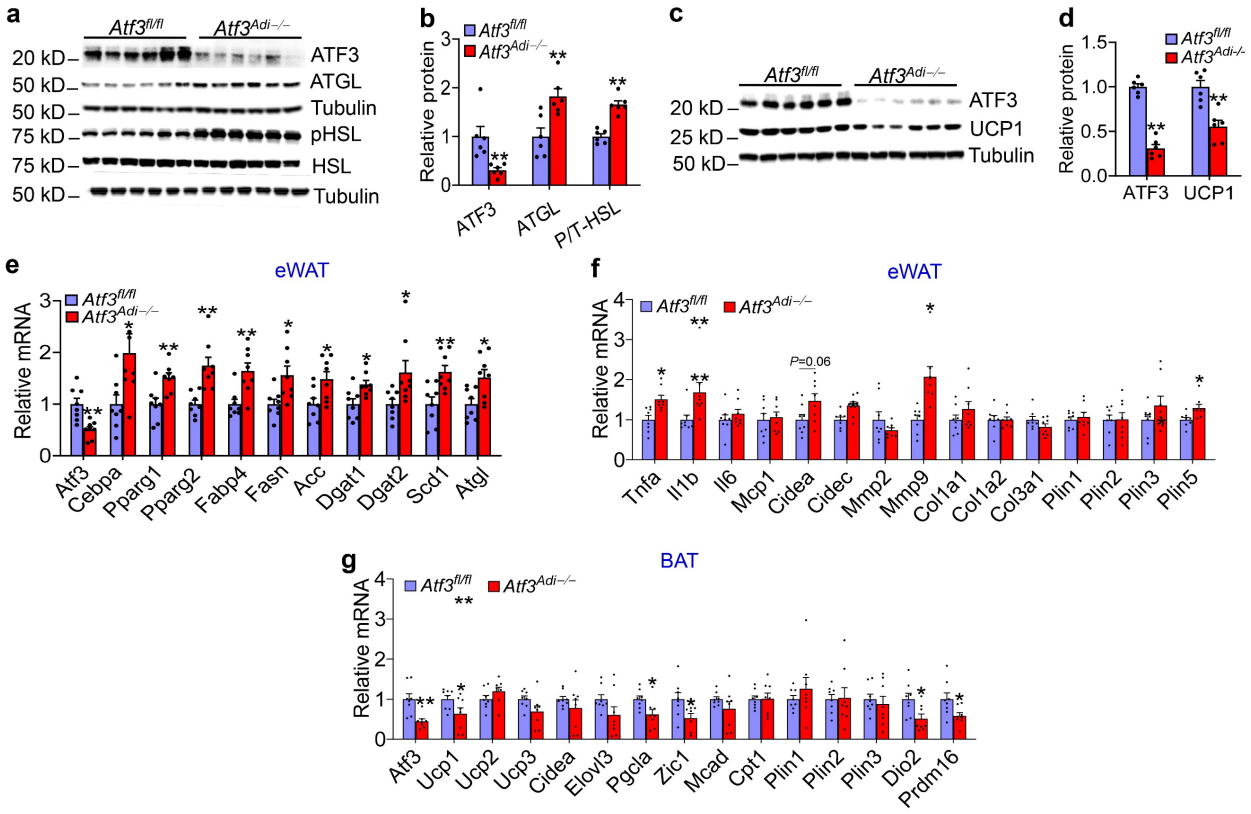

Supplementary Fig. 8. Effect of adipocyte ATF3 ablation on adipose gene expression in high fat diet-fed mice. *Aft3*$^{fl/fl}$ mice and *Atf3*$^{Adi-/-}$ mice were fed a high fat diet for 16 weeks (n=8 per group). **a-b** Protein levels in eWAT. **c-d** Protein levels in BAT. **e-f** mRNA levels in eWAT. **g** mRNA levels in BAT. Data are expressed as mean±SEM. Statistical analysis was performed using a 2-tailed, unpaired *t*-test (**b, d, e-g**). **P*<0.05, ***P*<0.01 versus controls

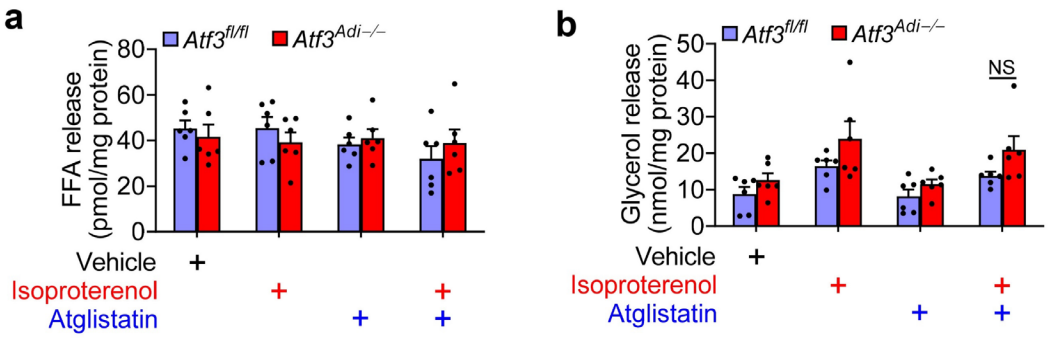

Supplementary Fig. 9. Loss of adipocyte ATF3 does not affect lipolysis at the basal levels. Lipolysis was performed under the basal conditions (0 h) using adipose tissue isolated from *Atf3*$^{fl/fl}$ or *Atf3*$^{Adi-/-}$ mice. FFA (**a**) or glycerol (**b**) release was determined (n=6). Data are expressed as mean±SEM. Statistical analysis was performed using two-way ANOVA (**a, b**). NS, not significant.

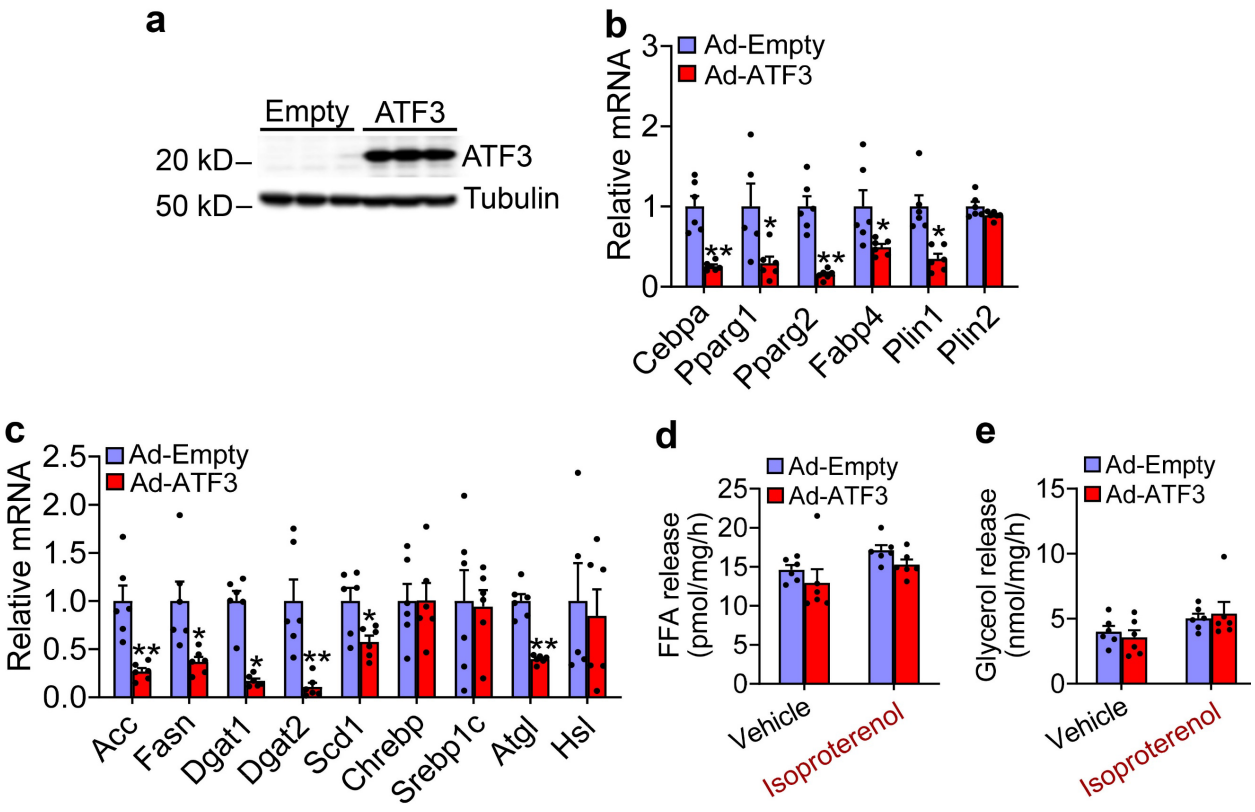

Supplementary Fig. 10. Effect of ATF3 over-expression on adipogenic and lipogenic genes and lipolysis in 3T3-L1 cells. a-e 3T3-L1 cells were infected with Ad-Empty or Ad-ATF3 and then differentiated to adipocytes in the presence of the hormonal cocktail (n=6). Protein (**a**) and mRNA (**b-c**) levels were determined. FFA (**d**) or glycerol (**e**) release under the basal conditions (0 h) was determined (n=6). Data are expressed as mean±SEM. Statistical analysis was performed using a 2-tailed, unpaired *t*-test (**b-c**) or two-way ANOVA (**d-e**). **P*<0.05, ***P*<0.01

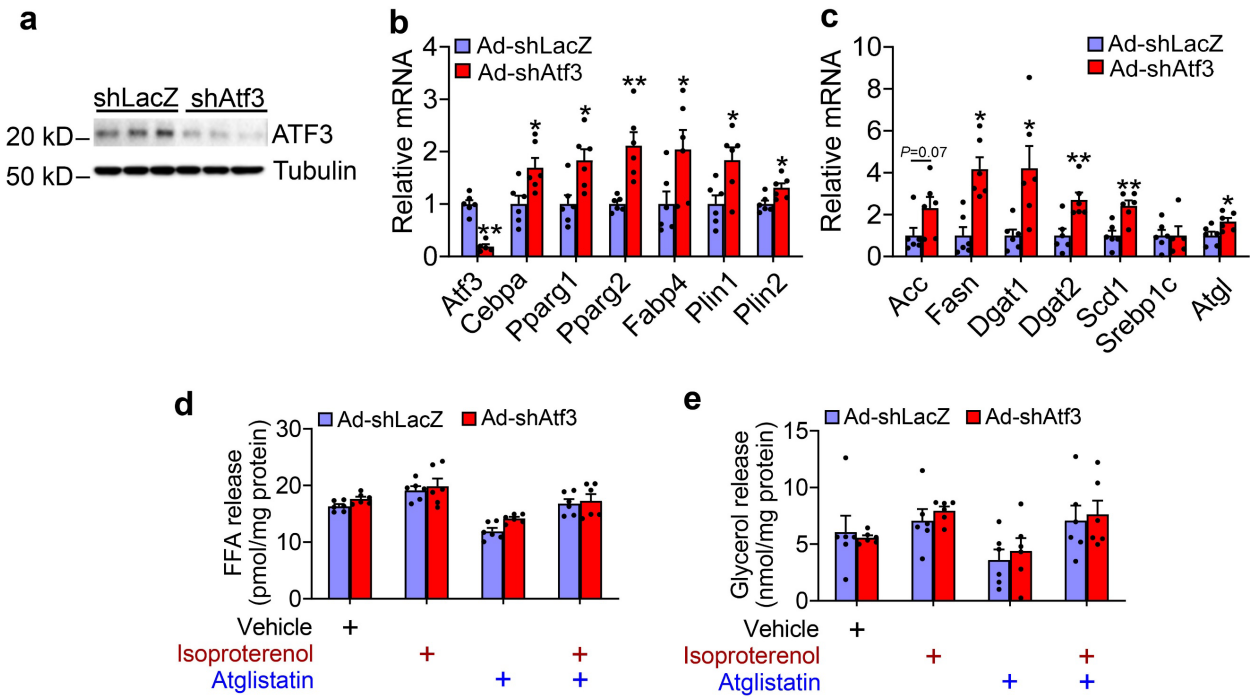

Supplementary Fig. 11. Effect of ATF3 knockdown on adipogenic and lipogenic genes and lipolysis in 3T3-L1 cells. a-e 3T3-L1 cells were infected with Ad-shLacZ or Ad-shAtf3 and then differentiated into adipocytes in the presence of the hormonal cocktail (n=6). Protein (**a**) and mRNA (**b-c**) levels were determined. FFA (**d**) or glycerol (**e**) release under the basal conditions (0 h) was determined (n=6). Data are expressed as mean±SEM. Statistical analysis was performed using a 2-tailed, unpaired *t*-test (**b-c**) or two-way ANOVA (**d-e**). **P*<0.05, ***P*<0.01

Uncut gel images

Fig. 1b

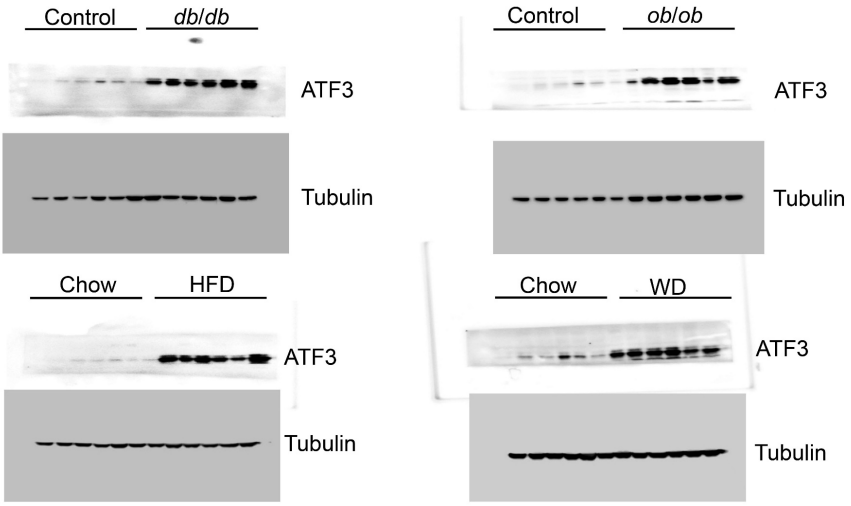

Fig. 1h

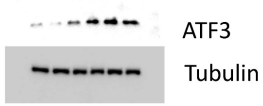

Fig. 1k

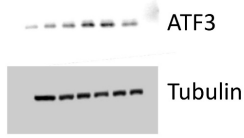

Fig. 1n

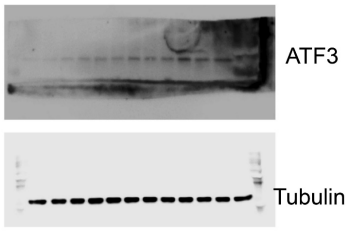

Fig. 2j

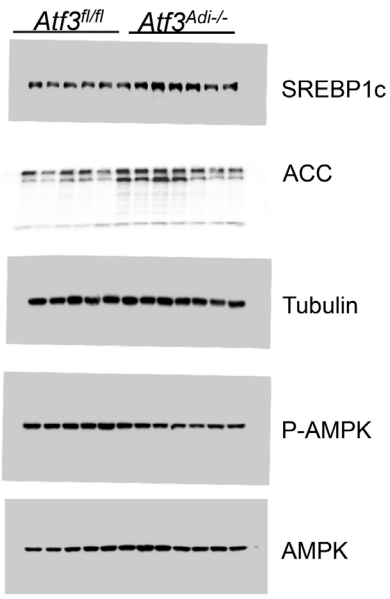

Fig. 3i

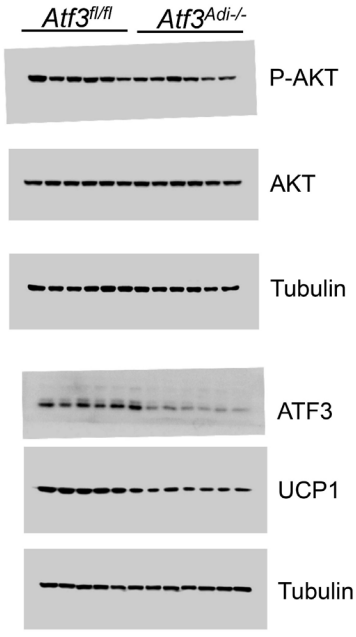

Fig.5a

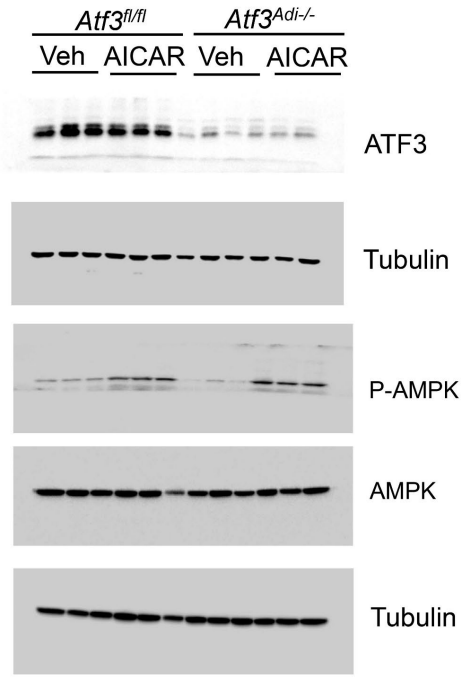
Atf3fl/fl
Atf3Adi-/-
Veh
AICAR
Veh
AICAR
ATF3
Tubulin
P-AMPK
AMPK
Tubulin

Fig.5m

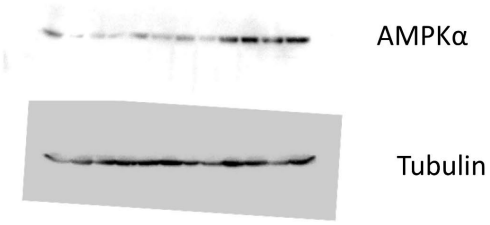
AMPKα
Tubulin

Uncut gel images

Supplemental Fig. 1a

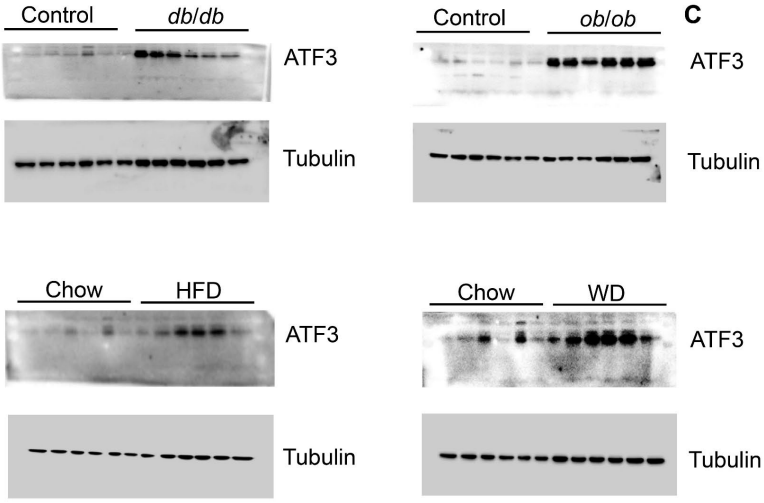

Supplemental Fig. 1c

Supplemental Fig. 3a

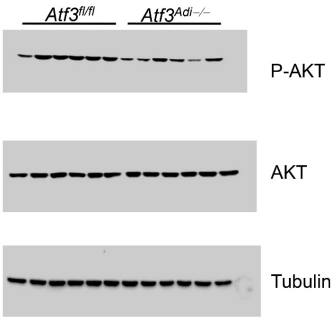

Supplemental Fig. 3c

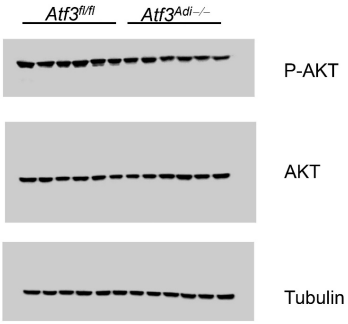

Supplemental Fig. 3e

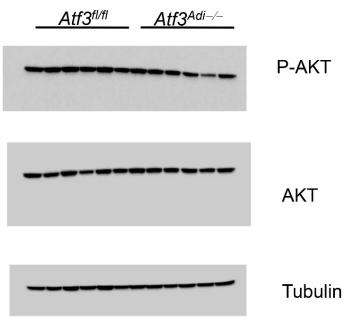

Uncut gel images

Supplemental Fig. 5l

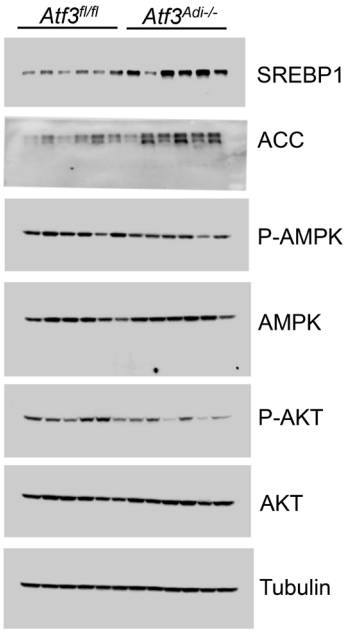

Supplemental Fig. 6a

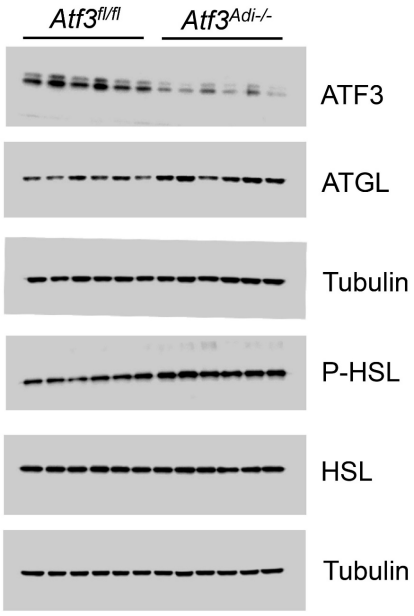

Supplemental Fig. 6c

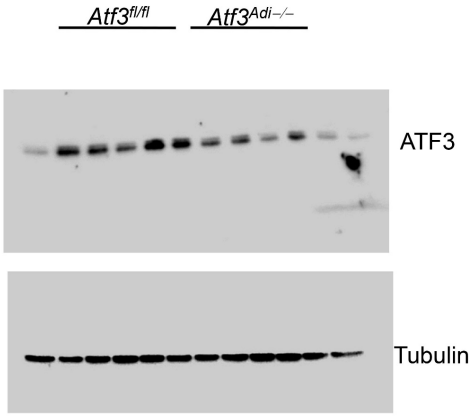

Uncut gel images

Supplemental Fig. 7k

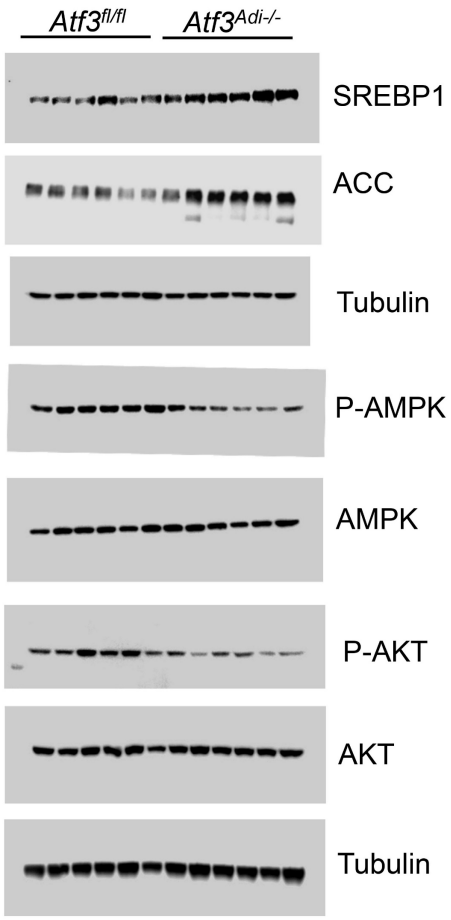

Uncut gel images

Supplemental Fig. 8a

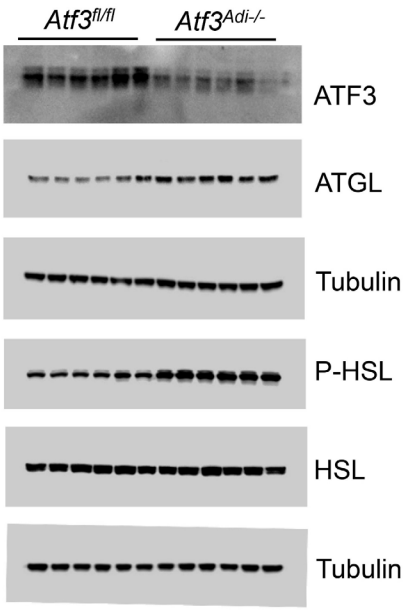

Supplemental Fig. 8c

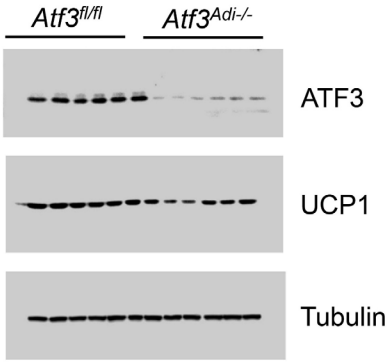

Supplemental Fig. 10a

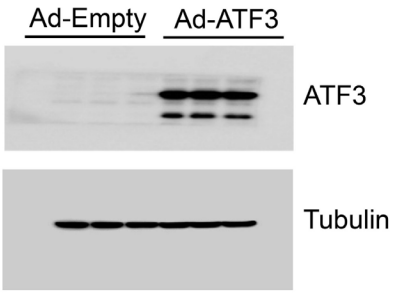

Supplemental Fig. 11a